🔓 **Open Access**

Reduction of Flicker Phase Noise in High-Speed Photodetectors Under Ultrashort Pulse Illumination

Dahyeon Lee
Takuma Nakamura
Jizhao Zang
Joe C. Campbell, *Fellow, IEEE*
Scott A. Diddams, *Senior Member, IEEE*
Franklyn Quinlan, *Senior Member, IEEE*
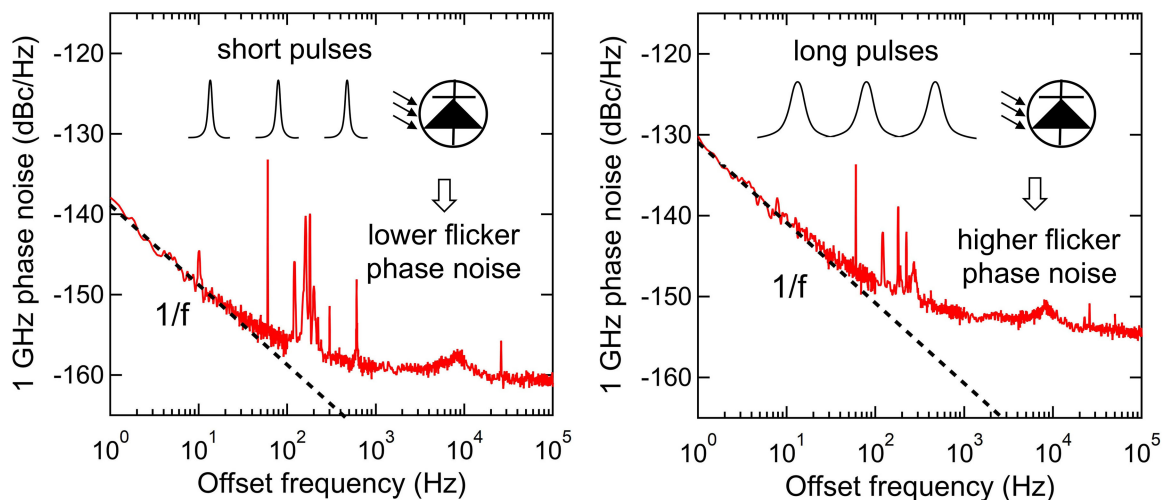
Reduction of Flicker Phase Noise in High-Speed Photodetectors Under Ultrashort Pulse Illumination

Dahyeon Lee [iD],[1,2] **Takuma Nakamura** [iD],[1,2] **Jizhao Zang** [iD],[3]
Joe C. Campbell [iD],[3] *Fellow, IEEE,*
Scott A. Diddams [iD],[1,2] *Senior Member, IEEE,*
and Franklyn Quinlan [iD],[1,2] *Senior Member, IEEE*

[1]Department of Physics, University of Colorado Boulder, Boulder, CO 80309 USA
[2]Time and Frequency Division, National Institute of Standards and Technology, Boulder, CO 80305 USA
[3]Department of Electrical and Computer Engineering, University of Virginia, Charlottesville, VA 22904 USA

Abstract: High-fidelity photodetection enables the transfer of the low noise inherent to optical oscillators to the microwave domain. However, when photodetecting optical signals of the highest timing stability, photodiode flicker (1/f) noise can dominate the resulting timing jitter at timescales longer than ~1 ms. With the goal of improving femtosecond-level timing fidelity when transferring from the optical to microwave domain, we vary the duty cycle of a train of optical pulses and show that the photodetector flicker phase noise on a photonically generated 1 GHz microwave signal can be reduced by ~10 dB under ultrashort pulse illumination, reaching as low as −140/f dBc/Hz. In addition, a strong correlation between amplitude and phase flicker noise is found, implying a single baseband noise source can modulate both quadratures of the microwave carrier. These findings expand the limits of the ultimate timing stability that can be transferred from optics to electronics.

Index Terms: 1/f noise, microwave phase noise, photodiodes.

1. Introduction

Photonic systems offer a compelling solution for microwave signal generation, processing, and dissemination thanks to the low noise of optical sources, the broad bandwidth supported by optical fiber and components, and the ability to transmit over large distances with extremely low loss [1]. Indeed, photonics can outperform traditional microwave techniques in areas such as low noise signal generation [2]–[6], timing synchronization [7], [8], arbitrary waveform generation [9], and high-speed signal processing [10], [11]. In such applications, high-fidelity optical-to-electrical conversion is nearly always required such that the microwave signal that has been generated or processed optically can be delivered to the end user. It is therefore valuable to characterize the noise and nonlinearities inherent in photodetection.

An important subset of photonic links requires high-fidelity detection of ultrashort optical pulses. For example, generating ultrastable microwaves with instability below 10^{-15} at 1 second derived

from optical atomic clocks and oscillators entails photodetection of optical pulse trains with femtosecond timing jitter [2]–[4]. In addition to contending with the nonlinearity of detecting high peak powers [12]–[15], transferring the exquisite timing available from optical sources to the microwave domain is extremely sensitive to excess noise such as photocurrent shot noise and flicker noise. Of these, flicker noise is least well understood [16]–[18], and it is the largest noise contributor to optical-to-microwave frequency down-conversion for timescales longer than ~1 ms. As optical clock performance continues to improve, finding ways to mitigate photodetector flicker noise in photonic microwave generation gains importance.

Here we explore how photodiode flicker noise is transferred from near baseband to the microwave carrier, with the aim of finding ways to reduce the impact of flicker on the phase noise of photonically generated microwave signals. By varying the temporal width of the optical pulses illuminating a photodiode, we manipulate the mapping of photodiode flicker noise onto microwave phase and amplitude. We find the phase noise component of the flicker noise is reduced when detecting short pulses by as much as 10 dB, reaching below $-140/f$ dBc/Hz on a 1 GHz carrier, with corresponding fractional frequency instability below $1 \times 10^{-16}/\tau$. This behavior is explained with a cyclostationary noise model with good agreement between the measured and predicted phase noise reduction. In addition, we show that the amplitude and phase flicker noise are highly correlated, and we present how this correlation impacts noise measurements. To our knowledge these are the first experimental demonstrations of flicker phase noise reduction by using ultrashort pulses, and the first demonstration that photodiode flicker noise is correlated between amplitude and phase quadratures.

In the following section, we introduce the simple models through which we interpret the imbalance between the flicker amplitude and phase levels, and how we expect correlated amplitude and phase flicker noise to impact our measurements. The experimental setup is then explained in Section 3, followed by measurement results in Section 4 and conclusions in Section 5.

2. Empirical Noise Models

The amount of flicker noise that a photodiode imposes on a photonically generated microwave carrier is determined by two distinct effects. First is the semiconductor physics that leads to the ~1/f behavior in the noise power spectral density at frequencies near DC [19]–[22]. While no comprehensive model for the physical origins of flicker noise in high-speed photodetectors has been proposed, carrier trapping and de-trapping [23], mobility fluctuation, and charge carrier number fluctuation [20] are generally accepted as important contributors. Second, when the photodetector is illuminated by a time-varying optical power, this noise modulates the amplitude and phase of the generated microwave signals, essentially up-converting the near-DC flicker noise into near-carrier noise. This noise up-conversion process may originate from the modulation of one or more parameters of the detector. For example, noise on a voltage source used to bias a photodiode, including flicker, will modulate the electric field in the detector, and in turn the microwave phase and amplitude. Importantly, the flicker noise is proportional to the square of the photocurrent [21], [24]. Therefore, in the detection of optical pulses, flicker noise only exists over the duration of the photocurrent pulse. (This is in contrast to thermal noise, which is present at all times regardless of whether photocurrent pulses are present.) As described in Section 2.1, the nonstationary nature of the flicker noise implies the relative level of the amplitude and phase noise is dependent on the width of the current pulse. Furthermore, if the noise is derived from a single baseband phenomenon, the amplitude and phase noise are expected to be correlated. Ramifications of correlated amplitude and phase are described in Section 2.2.

2.1 Pulse Width Dependence

When photodetecting optical pulse trains, noise processes that are only present over the duration of a pulse are cyclostationary, *i.e.*, the noise statistics, such as mean and variance, are periodic in time [25]. In addition to flicker noise, examples include shot noise [26], [27], and signal-spontaneous beat
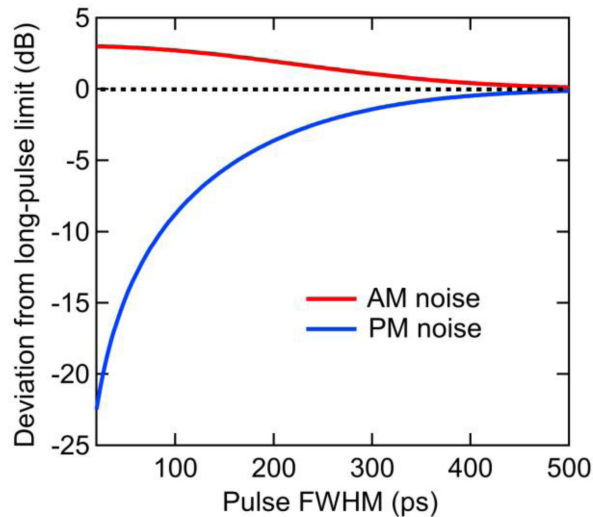
Fig. 1. Expected distribution of flicker noise in amplitude and phase quadratures on a 1 GHz carrier for a train of Gaussian pulses, as computed from (1) and (2). In the long-pulse limit, AM and PM noise have equal magnitudes. For short pulses, the AM noise is increased by up to 3 dB, whereas the PM noise is significantly reduced.

noise from optical amplifiers [28], [29]. In reference [27], an analytical cyclostationary model was presented that predicted that short pulse detection will lead to an imbalance of amplitude and phase noise arising from photocurrent shot noise. While there are important differences between shot noise and flicker noise, the shared cyclostationary nature of the noise sources suggests we may still determine the imbalance between amplitude and phase flicker noise based on the development in [27].

When detecting short pulses with a repetition rate of f_{rep}, the photodetector produces photocurrent at frequencies nf_{rep}, where n is a positive integer. The photodetection noise manifests as noise sidebands at $nf_{rep} \pm \delta f$, each of which is divided between amplitude modulation (AM) noise and phase modulation (PM) noise. From [27], the amplitude and phase noise power spectral densities arising from a cyclostationary process are given by

$$L_{AM(PM)}(f) = (1 \pm C)\, L_{avg}(f). \tag{1}$$

Here, the plus (minus) sign corresponds to AM (PM) noise, $L_{avg}(f)$ is the average of AM and PM noise power spectral density, and C gives the imbalance between the amplitude and phase noise, expressed as

$$C = \frac{I(2nf_{rep})}{I(0)}. \tag{2}$$

In (2), $I(2nf_{rep})$ is the magnitude of the Fourier transform of the photocurrent pulse at twice the frequency of interest and $I(0)$ is the value at 0 Hz. In the limit of infinitely short pulses, all the peaks at integer multiples of f_{rep} have equal heights in the frequency domain, resulting in $C = 1$. In this case, the noise completely resides in the amplitude quadrature. For nonzero pulse widths, $I(2nf_{rep})$ is less than $I(0)$, yielding a C that is less than 1, and some fraction of the noise in the phase quadrature. When $C \approx 0$, corresponding to long pulse widths, the noise is distributed equally between amplitude and phase quadratures.

Expected deviations of AM and PM noise from this long-pulse limit on a 1 GHz carrier is plotted in Fig. 1 for a train of Gaussian shaped pulses. For each pulse width, we computed C by taking the Fourier transform of the pulse shape and using (2). Equation (1) then gives the expected magnitudes of AM and PM noise. Note that the separation of AM and PM is different for different

pulse shapes, even with the same FWHM. We experimentally observed that, after taking into consideration the detailed pulse shape, the distribution of flicker noise between amplitude and phase noise closely follows what is expected from this model (Section 4.1).

It is important to note that the presented model only tells us the separation between AM and PM, not the absolute level. It is interesting to consider if the absolute level of L_{avg} can change as a function of pulse width as well. Nonlinearity as measured by amplitude-to-phase (AM-to-PM) noise conversion is known to change with pulse width [30], and it is possible that the DC flicker level can vary, similar to what has been observed in MOS transistors with modulated bias [31]. Section 4.1 presents experimental evidence that under certain conditions, L_{avg} does indeed change.

2.2 Correlation of Amplitude and Phase Flicker Noise

An experimental demonstration of correlated amplitude and phase flicker noise from a photodiode could provide insight into the physical origins of the flicker noise. More than this, proper determination of the imbalance between L_{AM} and L_{PM} must take into consideration whether the amplitude and phase flicker noise are correlated. To see this, consider a microwave signal under test with amplitude noise $a(t)$ and phase noise $\phi(t)$:

$$[1 + a(t)] \cos\left[2\pi n f_{rep} t + \phi(t)\right]. \tag{3}$$

Measurement entails comparing (multiplying) this signal with a reference signal $\cos(2\pi n f_{rep} + \Phi_r)$, where the demodulation angle Φ_r determines whether the extracted noise is amplitude noise, phase noise, or a combination of both. Experimentally, the multiplication happens at a mixer and Φ_r is set by a phase shifter. When $\Phi_r = 0$ the demodulated signal is proportional to $a(t)$ and when $\Phi_r = \pi/2$ the mixer output is proportional to $\phi(t)$. In general, the mixer output is proportional to (after low-pass filtering and AC coupling) [32]

$$a(t) \cos \Phi_r + \phi(t) \sin \Phi_r. \tag{4}$$

Both $a(t)$ and $\phi(t)$ are complicated functions of time, but it is instructive to consider amplitude and phase modulation at a single frequency ω_m. The results of this analysis can be generalized to all modulation frequencies when $a(t)$ and $\phi(t)$ are both much less than one. When $a(t)$ and $\phi(t)$ are correlated, there is a fixed phase relationship between the two. In other words, if we express the amplitude modulation as

$$a(t) = A_{AM} \cos(\omega_m t), \tag{5}$$

then there is some constant relative angle θ such that the phase modulation is given by

$$\phi(t) = A_{PM} \cos(\omega_m t + \theta). \tag{6}$$

Demodulation by the reference signal can be interpreted as a projection of the noise onto a line in the IQ plane (Fig. 2(a)). Therefore, by demodulating correlated AM and PM noise we take the projection of the vector sum of $a(t)$ and $\phi(t)$ onto the line defined by Φ_r.

When $a(t)$ and $\phi(t)$ are correlated, the vector sum traces out an ellipse with a period of $2\pi/\omega_m$. The shape of the ellipse is determined by A_{PM}/A_{AM} and θ. Examples of some special cases are shown for different values of A_{PM}/A_{AM} and θ in Fig. 2(b)-(d). Note that when $\theta = 0$, corresponding to the case when amplitude and phase noise are in phase, the demodulated signal is very small for certain demodulation angles, namely when

$$\Phi_{r,min} = \arctan(A_{PM}/A_{AM}) + (\pi/2 \text{ or } 3\pi/2). \tag{7}$$

More generally, when $\theta = 0$ the demodulated power at ω_m as a function of angle Φ_r is proportional to

$$\left(A_{AM}^2 + A_{PM}^2\right) \sin^2\left(\Phi_r - \Phi_{r,min}\right). \tag{8}$$

Thus, when the AM and PM are correlated with $\theta = 0$, a low noise output can be found for any ratio of AM to PM simply by tuning to the correct demodulation angle. Precise knowledge of the
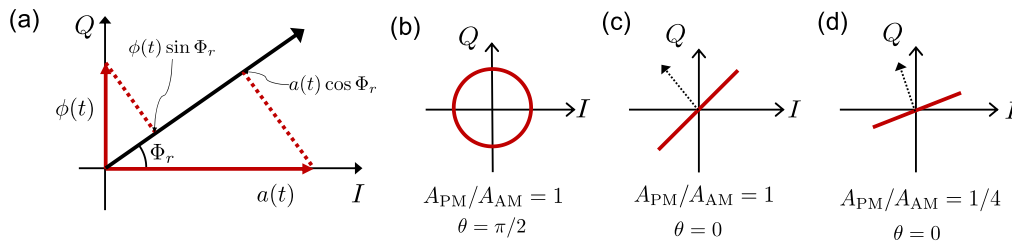
Fig. 2. Demodulation of correlated amplitude and phase noise. (a) The process of noise demodulation can be considered as a projection onto a line in the IQ plane defined by the demodulation angle Φ_r. (b)–(d) Example IQ plane representations for correlated AM and PM for different AM/PM ratios and relative angle θ. When amplitude and phase noise are correlated, the vector sum of the combined noise traces out an ellipse in general. When $\theta = 0$, the vector sum traces out a line, and the demodulated signal can be very small for certain demodulation angles (shown with dotted arrows).
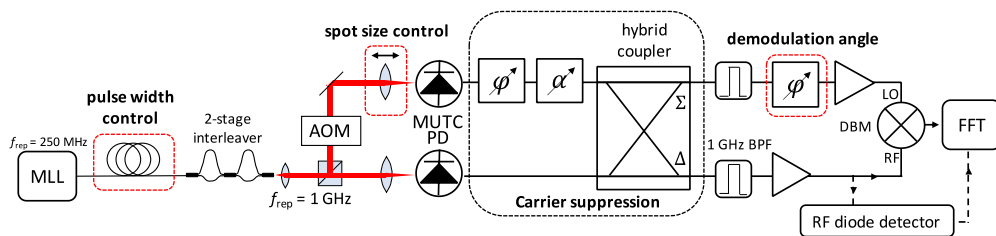
Fig. 3. Experimental setup. Two 1 GHz tones derived from a common source are compared with each other for the measurement of photodetection noise. Control parameters in the experiment are highlighted with red dotted boxes. MLL: Modelocked laser; AOM: Acousto-optic modulator; MUTC PD: Modified uni-traveling carrier photodiode; α: Variable attenuator; ϕ: Variable phase shifter; BPF: Band-pass filter; DBM: Double balanced mixer; FFT: Two-channel fast Fourier transform spectrum analyzer.

demodulation angle is therefore important to avoid underreporting the phase or amplitude noise. In Section 4.2, we show the amplitude and phase noise are correlated with $\theta = 0$, and further show that the demodulation angle that gives the lowest noise is consistent with the separately measured ratio A_{PM}/A_{AM}.

3. Experimental Setup

A schematic of the photodiode flicker noise measurement system is shown in Fig. 3. Two 1 GHz tones were derived from a common optical source and compared. The optical source consisted of an Er:fiber mode-locked laser with repetition rate of 250 MHz, followed by dispersive optical fiber, added in 50 m increments, to control the optical pulse width. The native repetition rate of the mode-locked laser was increased to 1 GHz by way of a 2-stage optical pulse interleaver. The inclusion of the pulse interleaver increases the microwave saturation power and improves detector linearity by reducing the energy per incident pulse [29], [33]. After the interleaver, pulses were launched into free-space and directed onto two modified uni-traveling carrier (MUTC) photodiodes designed for high linearity and high power, with active regions of 34 μm and 50 μm [34], [35]. An acousto-optic modulator was placed in the beam path prior to the 50 μm detector, where the 0th order output was used to modulate the pulse energy for demodulation angle calibration. Focusing lenses controlled the optical spot size on the detectors. The MUTC photodiodes generated a series of electrical pulses with an average photocurrent of 2 mA under -8 V bias. In the frequency domain, this corresponds to an array of tones at integer multiples of the pulse repetition frequency. A single tone (1 GHz in our case) was selected from each photodetected signal for measurement. At 2 mA

of average photocurrent, the power of the 1 GHz tone was -4 dBm and -6 dBm for short and long pulses, respectively.

In anticipation of very low flicker noise levels [16], [17], an interferometric carrier suppression method [36], [37] was used to measure the amplitude and phase noise of the 1 GHz signals. The interferometer arms consisted of the two signal paths beginning at the optical beam splitter and ending at the microwave hybrid coupler. The phase and amplitude of the microwave signal in one path was adjusted such that the 1 GHz carrier in the "dark" port (Δ) was suppressed by >60 dB. Carrier suppression results in a commensurate reduction of the flicker noise contribution from subsequent microwave components such as amplifiers and mixers [16]. The overall effect of the interferometric carrier suppression is amplification of the photodiode flicker with substantially less added noise close to carrier. The measurement noise floor was obtained by splitting the common signal from one photodiode in the interferometer. The noise floor level was insensitive to the demodulation angle. As shown below, this floor was low enough to reveal the desired photodiode flicker noise.

For noise demodulation, the 1 GHz signals from the dark and bright (Σ) ports of the interferometer were multiplied with each other at the mixer, and the mixer output was low-pass filtered. The resulting baseband signal was sent to a fast Fourier transform (FFT) spectrum analyzer for analysis. A phase shifter placed before the mixer was used to set the noise demodulation angle. This phase shifter was first calibrated to a demodulation angle of 90° by suppressing the amplitude modulation tone imposed by the AOM. Other demodulation angles were reached by adjusting the phase shifter knob by a calibrated number of turns. Noise levels were calibrated via the single sideband method [38].

In order to measure the correlation between AM and PM flicker noise, another branch dedicated for AM measurement was added. The interferometer dark port output was split, part of which was amplified (not shown in Fig. 3), and then directed to an RF diode detector. The AM noise measured with the diode detector and simultaneously measured PM noise were sent to a two-channel FFT spectrum analyzer to compute the cross spectral density and phase. We note that the agreement between the AM noise measured with the RF diode detector and from the mixer with 0° demodulation angle was excellent.

Since these measurements required high sensitivity at small offset frequencies, abundant care was taken to make sure that environmental noise or the measurement system itself did not corrupt the data or lead to its misinterpretation. As noted in [16], it is very easy to mistake technical noise for photodiode flicker noise. Here we list some potential noise sources that could have otherwise spoiled the integrity of data and the precautions we took against them.

The optical pulse source has intensity and timing fluctuations far above the level of measured photodiode flicker noise, with a relative intensity noise (RIN) of -110 dB/Hz at 10 Hz offset frequency and a timing jitter noise corresponding to -35 dBc/Hz at 10 Hz offset frequency on a 1 GHz carrier. However, the combination of the interferometric carrier suppression method and common mode rejection eliminates their effects on the final measurement [36]. The carrier suppression method not only suppresses the 1 GHz carrier, but also the amplitude and phase noise of the source oscillator at the same level of carrier suppression, >60 dB in our case. Thus, the remaining laser RIN is below -170 dB/Hz at 10 Hz, and has a negligible contribution to our amplitude noise measurements. The pulse-to-pulse timing noise of the optical source is further suppressed by the common-mode rejection at the mixer. Given the short path length difference between the two branches leading to the mixer in our experiment (<1 m), we estimate the common mode rejection of the source oscillator phase noise to be greater than 130 dB at 10 Hz offset frequency [39]. This doubly suppressed phase noise of the source, after >190 dB suppression, would show up at <-225 dBc/Hz at 10 Hz offset frequency in the final measurement, well below our measurement floor.

To ensure that AM-to-PM conversion effects do not lead to a misinterpretation of the data, for example, when calibrating the demodulation angle through minimization of the AOM tone, separate measurements of the AM-to-PM conversion ratio were taken [15]. For various pulse widths, photocurrents, and spot sizes used in the experiment, the AM-to-PM conversion ratio was

always less than -25 dB. This leads to a maximum error in the demodulation angle of less than $4°$. Moreover, this low AM-to-PM conversion, combined with the measurement system common mode rejection, results in negligible RIN impact on the phase noise measurements.

Various other measures were taken to strictly control experimental parameters, some of which turned out to be essential. To avoid noise generated by backscattering in the fiber and at fiber interfaces [40], [41], optical isolators were added at each end of the dispersive broadening fiber and most fiber connections were spliced. All fibers were taped down to prevent polarization drifts. All free-space optics were doubly enclosed to avoid alignment fluctuations due to air currents, as well as for acoustic isolation. Microwave isolators were inserted at various points such that back reflections could not perturb the carefully set carrier suppression. Frequency diplexers were placed immediately after each bias tee to separate repetition rate harmonics >4GHz, which were subsequently terminated into 50 Ohms, to minimize their back reflection to the photodiode. Moreover, the use of the pulse interleaver reduced unwanted repetition rate harmonics by more than 25 dB, minimizing their back reflection to the photodiode. The photodiodes were mounted on temperature-controlled heat sinks. Measurements were taken when there was no human activity nearby, with the experimenter initiating the measurement >1m away.

4. Results and Discussion

4.1 Pulse Width Dependence

Electrical pulses from the 50 μm MUTC detector for various amounts of dispersive fiber broadening are shown in Fig. 4(a). Without any additional optical fiber, the MUTC photodiodes produced impulse response-limited electrical pulses with a full width at half maximum (FWHM) of 30 ps. The addition of extra fiber lengths of 100 m, 200 m, or 300 m broadened the photodetected electrical pulses to a FWHM of 80 ps, 140 ps, and 190 ps.

Phase and amplitude noise for the shortest and longest pulse durations are shown in Figs. 4(b) and 4(c). As expected from the cyclostationary model, a large separation between AM and PM flicker noise of about 10 dB was observed for the shortest pulses. In contrast, for the longest pulses, the noise was distributed almost evenly between AM and PM. For pulse widths in between these two extremes, the separation of AM and PM flicker noise was intermediate, as shown in Fig. 5(a). The expected separation of AM and PM based on (1) is represented by the shaded region, in good agreement with the experimental results. Since, as stated above, the model only predicts the ratio of AM and PM values and not the absolute level, the center of the shaded region was chosen to lie on $\sqrt{L_{AM}L_{PM}}$ for each pulse width.

To test the consistency of the results under other experimental conditions, the same measurement was repeated as the illumination spot size on one detector was changed by moving the focusing lens. Some representative results are shown in Fig. 5(b)–(d). The FWHM of the illumination spot was varied from 5 μm to 40 μm, where the maximum spot size of 40 μm corresponded to a lens displacement of 230 μm from the position that gave the smallest spot size. Shorter pulses produced a larger imbalance of AM and PM flicker for all illumination spot sizes. However, varying the illumination spot size revealed that the total flicker noise $L_{AM} + L_{PM}$ can change with the pulse width as well as with illumination spot size. This is most pronounced for 50 μm lens position where the shortest pulses do not yield the lowest flicker noise. This may be related to the changing photodiode nonlinearity associated with changing peak intensity, similar to how photodiode nonlinearity affects AM-to-PM conversion [15]. While the AM-to-PM conversion changes with pulse width and with spot size, no clear trend between lower AM-to-PM conversion and lower total flicker noise was observed. More investigation is needed to understand the variation in $L_{AM} + L_{PM}$.

The experimental data in Fig. 5 show that the cyclostationary noise model accurately describes the reduction of photodiode flicker phase noise when detecting short pulses. The reduction of phase noise by as much as 10 dB demonstrated here can be valuable for applications that call for precise reproduction of pulse timing such as optical frequency division. Indeed, these results may explain
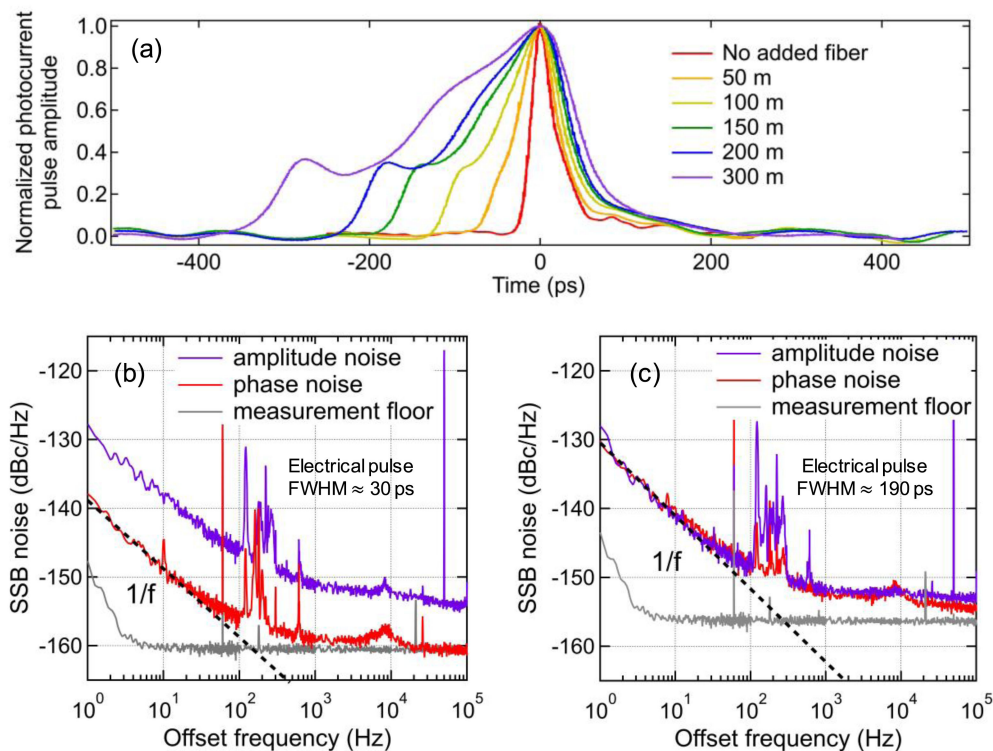
Fig. 4. Pulse widths and flicker noise on a 1 GHz carrier. Reported noise levels are for two photodetectors. (a) Normalized electrical pulses for different lengths of added fiber. (b) Amplitude and phase single sideband (SSB) flicker noise for short pulses (no added fiber). Phase noise is lower than amplitude noise by about 10 dB. (c) Amplitude and phase SSB flicker noise for long pulses (with 300 m added fiber). Amplitude and phase noise are at a comparable level. The higher measurement noise floor in (c) is largely due to the lower 1 GHz power in broad pulse detection. The strong tone at 50 kHz in the AM noise plots is the AM calibration tone applied to the AOM. Noise spikes between 100 Hz and 400 Hz are acoustic and seismic in origin.

why phase flicker levels nearing $-140/f$ dBc/Hz have been seen under short pulse detection [4], [17], [42], whereas phase flicker measurements under modulated CW light illumination have been 10 to 15 dB higher [16], [43], [44]. Further improvement in flicker phase noise can be expected for faster photodiodes that produce shorter impulse response-limited electrical pulses. For a given photodetector, it is better to use shorter pulses as long as detector saturation and nonlinearity do not pose limitations in achievable power or AM-to-PM conversion.

While the focus of this study has been the flicker noise, it is interesting to note that the AM and PM white noise levels follow a similar trend as a function of pulse width. The white noise levels are too high to be explained by either shot noise (maximum value below -160 dBc/Hz for the photocurrent and pulse widths used) or thermal noise (given by the measurement floor). We therefore assume the excess white noise to originate from baseband as well. Further evidence for this is the fact that the small noise peak around 8 kHz in Fig. 4(b) and (c) is also seen in the baseband voltage noise of the photodetector bias sources. In this case, we would expect the AM and PM white noise floors to follow the same pulse width dependence.

4.2 Correlation of Amplitude and Phase Flicker Noise

While investigating the imbalance of amplitude and phase flicker noise for short pulse detection, we found that for some demodulation angles, the measured flicker noise was lower than the flicker phase noise. An example is shown in Fig. 6, where the lowest level of flicker noise is at
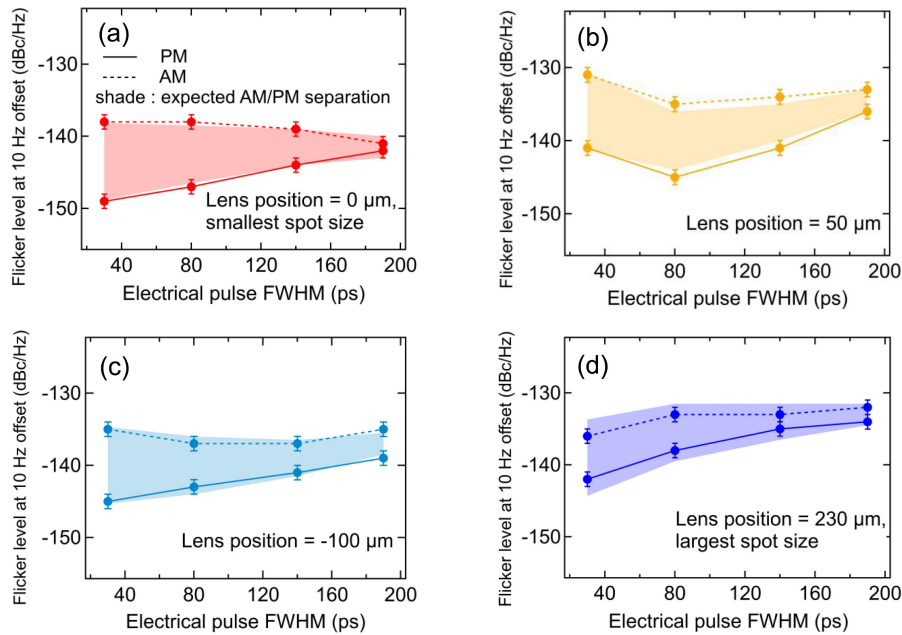
Fig. 5. Measured distribution of amplitude and phase flicker noise for various pulse widths and spot sizes. (a)–(d) The measured separation of AM and PM flicker noise matches the expected separation from (2) for all illumination spot sizes. Shorter pulses produced larger imbalance between AM and PM flicker noise. The illumination spot size was changed by displacing the focusing lens highlighted in Fig. 3. Error bars represent statistical uncertainty given by the variance in the flicker noise power spectral density.

a demodulation angle of 110°. This is a consequence of the correlation between amplitude and phase flicker noise. As discussed in Section 2.2, when AM and PM noise are correlated with a relative phase of $\theta = 0$ the demodulated noise can be very small at well-defined demodulation angles. Indeed, for the measured ratio of AM and PM noise, the demodulation angle of 110° is the special angle that produces low demodulated noise, provided that AM and PM are correlated with $\theta = 0$.

The phase relationship between AM and PM flicker was verified with a direct measurement of the relative angle via the cross spectrum. Fig. 7 shows the cross spectral density and phase from simultaneously measured photodiode AM and PM noise for short pulses and long pulses. For uncorrelated signals the cross spectral density averages to zero, and the phase is random [45]. Here however, the measured cross spectral density converges to a finite value, and the phase converges to 0°. This indicates a correlation between AM and PM noise, and that the correlated noise is in phase for both long and short pulses. In Fig. 7, the absolute level of the noise cross spectral density is chosen arbitrarily to be 0 dB/Hz at 1 Hz offset. Whereas this demonstrates the correlated noise close to carrier is of flicker type, we additionally use the coherence function $L_{AM, PM}/\sqrt{L_{AM}L_{PM}}$, where $L_{AM, PM}$ is the cross spectral density between AM and PM, as a measure of the strength of the correlation. This function ranges from a value of 1, corresponding to perfect correlation, to 0 for completely uncorrelated signals [25]. For the results presented in Fig. 7, the coherence function was above 0.7 in the flicker noise region between 1 Hz and 100 Hz for both short and long pulses, indicating strong coherence between amplitude and phase.

Once the magnitudes of AM and PM flicker noise and their relative phase are known, the flicker noise for any demodulation angle can be calculated from (8). Figs 7(c) and 7(d) show the measured flicker noise along with the prediction from (8) for different demodulation angles. The measured flicker noise closely follows the expected level, indicating that the low flicker at 110° demodulation
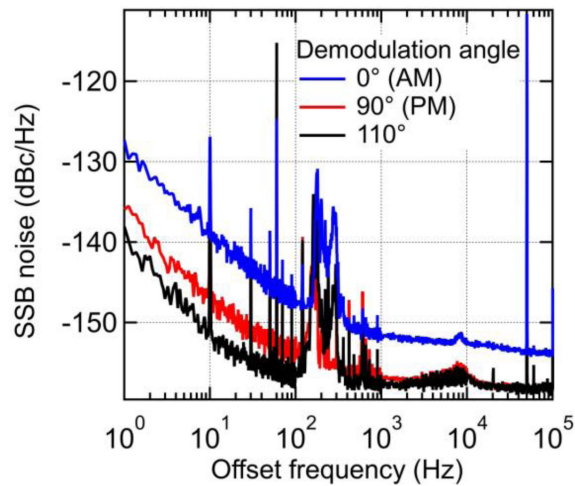
Fig. 6. Photodiode flicker noise for short pulse detection (∼30 ps electrical pulse FWHM) on 1 GHz carrier, measured for different demodulation angles. PM flicker noise is lower than AM flicker noise as expected from cyclostationary noise model. Flicker noise for a demodulation angle of 110° is even lower. This is due to the correlation between AM and PM flicker noise.
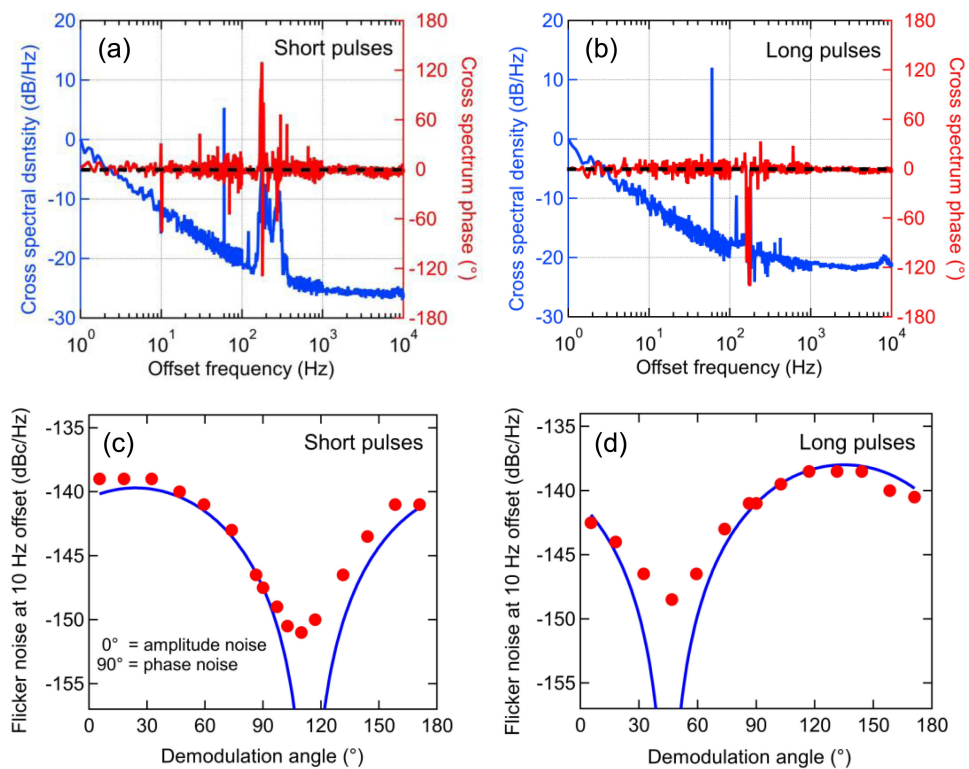
Fig. 7. Correlation between AM and PM flicker noise and its consequences. (a), (b), Cross spectral density and phase between AM and PM flicker noise for short and long pulses. In both cases, the cross-spectrum phase is constant, as opposed to random, indicating correlation between AM and PM flicker. The scale for the cross spectral density is chosen arbitrarily. (c), (d), Measured flicker noise level at 10 Hz offset (red dots) follows the prediction from equation (8) (blue lines), showing that the low flicker level at certain demodulation angles is due to the correlation between AM and PM flicker noise.

angle for short pulses is consistent with AM-PM correlation. For long pulses the minimum flicker shifts to a demodulation angle near $45°$ as a result of the smaller imbalance of L_{PM} and L_{AM}.

Similar AM-PM correlations have been found in RF oscillators [45], [46], diodes [47], and transistors [48], but to our knowledge, this is the first demonstration of AM-PM flicker correlation in photodiodes. While the origin of this correlation is not known, correlated AM-PM is consistent with the idea that a single baseband noise source will modulate both the amplitude and phase of a photonically generated microwave. Importantly, the AM-PM correlation can be of practical value for high-fidelity photodetection if the correlated AM is utilized to cancel the phase noise via feedforward. A 10 dB reduction of the phase noise of a microwave oscillator has been achieved with this method in [49].

5. Conclusion

Flicker noise in photonically generated 1 GHz microwave signals resulting from the detection of optical pulse trains has been shown to be unequally distributed between amplitude and phase quadratures. By measuring photodiode AM and PM flicker noise for different pulse widths, we observed ∼10 dB reduction in phase noise for short pulses, reaching −140/f dBc/Hz, in good agreement with a cyclostationary noise model. We also found strong correlation between AM and PM photodiode flicker noise, the first such demonstration in high-speed photodiodes. The AM-PM flicker correlation indicates a single baseband noise source can modulate both the amplitude and phase of a microwave carrier, and has the potential to be used to further suppress phase noise. These results provide valuable insight into the poorly understood photodiode flicker noise, and points to a convincing path toward very high-fidelity photodetection that can support optical clock stability beyond current state-of-the-art.

Acknowledgment

References

[1] J. Capmany and D. Novak, "Microwave photonics combines two worlds," *Nat. Photon.,* vol. 1, no. 6, pp. 319–330, 2007.
[2] T. M. Fortier *et al.*, "Generation of ultrastable microwaves via optical frequency division," *Nat. Photon.,* vol. 5, no. 7, pp. 425–429, 2011.
[3] T. Nakamura *et al.*, "Coherent optical clock down-conversion for microwave frequencies with 10^{-18} instability," *Science,* vol. 368, no. 6493, pp. 889–892, 2020.
[4] X. Xie *et al.*, "Photonic microwave signals with zeptosecond-level absolute timing noise," *Nat. Photon.,* vol. 11, no. 1, pp. 44–47, 2017.
[5] W. Liang *et al.*, "High spectral purity Kerr frequency comb radio frequency photonic oscillator," *Nat. Commun.,* vol. 6, no. 1, pp. 1–8, 2015.
[6] X. S. Yao and L. Maleki, "Optoelectronic microwave oscillator," *JOSA B,* vol. 13, no. 8, pp. 1725–1735, 1996.
[7] F. R. Giorgetta, W. C. Swann, L. C. Sinclair, E. Baumann, I. Coddington, and N. R. Newbury, "Optical two-way time and frequency transfer over free space," *Nat. Photon.,* vol. 7, no. 6, pp. 434–438, 2013.
[8] J. Kim, J. A. Cox, J. Chen, and F. X. Kärtner, "Drift-free femtosecond timing synchronization of remote optical and microwave sources," *Nat. Photon.,* vol. 2, no. 12, pp. 733–736, 2008.
[9] S. T. Cundiff and A. M. Weiner, "Optical arbitrary waveform generation," *Nat. Photon.,* vol. 4, no. 11, pp. 760–766, 2010.
[10] J. Capmany, J. Mora, I. Gasulla, J. Sancho, J. Lloret, and S. Sales, "Microwave photonic signal processing," *J. Lightw. Technol.,* vol. 31, no. 4, pp. 571–586, 2012.
[11] V. Torres-Company and A. M. Weiner, "Optical frequency comb technology for ultra-broadband radio-frequency photonics," *Laser Photon. Rev.,* vol. 8, no. 3, pp. 368–393, 2014.
[12] J. Taylor *et al.*, "Characterization of power-to-phase conversion in high-speed P-I-N photodiodes," *IEEE Photon. J.,* vol. 3, no. 1, pp. 140–151, Feb. 2011.
[13] W. Zhang, T. Li, M. Lours, S. Seidelin, G. Santarelli, and Y. Le Coq, "Amplitude to phase conversion of InGaAs pin photo-diodes for femtosecond lasers microwave signal generation," *Appl. Phys. B,* vol. 106, no. 2, pp. 301–308, 2012.
[14] R. Bouchand, D. Nicolodi, X. Xie, C. Alexandre, and Y. Le Coq, "Accurate control of optoelectronic amplitude to phase noise conversion in photodetection of ultra-fast optical pulses," *Opt. Exp.,* vol. 25, no. 11, pp. 11268–11281, 2017.

[15] J. Davila-Rodriguez *et al.*, "Optimizing the linearity in high-speed photodiodes," *Opt. Exp.,* vol. 26, no. 23, pp. 30532–30545, 2018.

[16] E. Rubiola, E. Salik, Y. Nan, and L. Maleki, "Flicker noise in high-speed p-i-n photodiodes," *IEEE Trans. Microw. Theory Techn.,* vol. 54, no. 2, pp. 816–820, Feb. 2006.

[17] F. N. Baynes *et al.*, "Attosecond timing in optical-to-electrical conversion," *Optica,* vol. 2, no. 2, pp. 141–146, 2015.

[18] O. Llopis, S. Azaizia, K. Saleh, A. A. Slimane, and A. Fernandez, "Photodiode 1/f noise and other types of less known baseband noises in optical telecommunications devices," in *22nd Int. Conf. Noise Fluctuations*, 2013, pp. 1–4.

[19] A. Hajimiri and T. H. Lee, "A general theory of phase noise in electrical oscillators," *IEEE J. Solid-State Circuits,* vol. 33, no. 2, pp. 179–194, Feb. 1998.

[20] F. N. Hooge, "1/f noise sources," *IEEE Trans. Electron. Devices,* vol. 41, no. 11, pp. 1926–1935, Nov. 1994.

[21] S. Kogan, *Electronic Noise and Fluctuations in Solids*. Cambridge U.K.: Cambridge Univ. Press, 2008.

[22] M. B. Weissman, "1/f noise and other slow, nonexponential kinetics in condensed matter," *Rev. Modern Phys.,* vol. 60, no. 2, pp. 537–571, 1988.

[23] A. McWhorter, "1/f noise and germanium surface properties," *Semicond. Surf. Phys.*, vol. 1057, pp. 207–228, 1957.

[24] L. He, Y. Lin, A. V. Rheenen, A. V. D. Ziel, A. Young, and J. V. D. Ziel, "Low-frequency noise in small InGaAs/InP p-i-n diodes under different bias and illumination conditions," *J. Appl. Phys.,* vol. 68, no. 10, pp. 5200–5204, 1990.

[25] W. A. Gardner, *Introduction to random processes with applications to signals and systems*. New York, NY, USA: MacMillan Co.*,* 1986.

[26] F. Quinlan *et al.*, "Exploiting shot noise correlations in the photodetection of ultrashort optical pulse trains," *Nat. Photon.,* vol. 7, no. 4, pp. 290–293, 2013.

[27] F. Quinlan, T. M. Fortier, H. Jiang, and S. A. Diddams, "Analysis of shot noise in the detection of ultrashort optical pulse trains," *JOSA B,* vol. 30, no. 6, pp. 1775–1785, 2013.

[28] V. S. Grigoryan, C. R. Menyuk, and R. M. Mu, "Calculation of timing and amplitude jitter in dispersion-managed optical fiber communications using linearization," *J. Lightw. Technol.,* vol. 17, no. 8, pp. 1347–1356, 1999.

[29] F. Quinlan *et al.*, "Optical amplification and pulse interleaving for low-noise photonic microwave generation," *Opt. Lett.,* vol. 39, no. 6, pp. 1581–1584 Mar. 2014.

[30] Y. Hu *et al.*, "Computational study of amplitude-to-phase conversion in a modified unitraveling carrier photodetector," *IEEE Photon. J.,* vol. 9, no. 2, Apr. 2017, Art. no. 5501111.

[31] S. L. Gierkink, E. A. Klumperink, A. P. V. D. Wel, G. Hoogzaad, E. A. V. Tuijl, and B. Nauta, "Intrinsic 1/f device noise reduction and its effect on phase noise in CMOS ring oscillators," *IEEE J. Solid-State Circuits,* vol. 34, no. 7, pp. 1022–1025, Jul. 1999, doi: 10.1109/4.772418.

[32] E. Rubiola and V. Giordano, "Phase noise metrology," in *Noise, Oscillators, and Algebraic Randomness*: Springer, 2000, pp. 189–215. [Online]. Available: https://www.springer.com/gp/book/9783662142967

[33] A. Haboucha *et al.*, "Optical-fiber pulse rate multiplier for ultralow phase-noise signal generation," *Opt. Lett.,* vol. 36, no. 18, pp. 3654–3656, 2011.

[34] A. Beling, X. Xie, and J. C. Campbell, "High-power, high-linearity photodiodes," *Optica,* vol. 3, no. 3, pp. 328–338, 2016.

[35] Z. Li *et al.*, "High-power high-linearity flip-chip bonded modified uni-traveling carrier photodiode," *Opt. Exp.,* vol. 19, no. 26, pp. B385–B390, 2011.

[36] E. N. Ivanov, M. E. Tobar, and R. A. Woode, "Microwave interferometry: Application to precision measurements and noise reduction techniques," *IEEE Trans. Ultrasonic., Ferroelect., Freq. Control,* vol. 45, no. 6, Nov. 1998, doi: 10.1109/58.738292.

[37] E. Rubiola and V. Giordano, "Advanced interferometric phase and amplitude noise measurements," *Rev. Sci. Instrum.,* vol. 73, no. 6, pp. 2445–2457, 2002.

[38] A. Hati, C. Nelson, N. Ashby, and D. Howe, "Calibration uncertainty for the NIST PM/AM noise standards," *NIST Special Pub. 250–90*, vol. 250, 2012.

[39] E. Rubiola, E. Salik, S. Huang, N. Yu, and L. Maleki, "Photonic-delay technique for phase-noise measurement of microwave oscillators," *J. Opt. Soc. Amer. B,* vol. 22, no. 5, pp. 987–997, 2005.

[40] M. Fleyer, S. Heerschap, G. A. Cranch, and M. Horowitz, "Noise induced in optical fibers by double Rayleigh scattering of a laser with a 1/f ν frequency noise," *Opt. Lett.,* vol. 41, no. 6, pp. 1265–1268, 2016.

[41] W. Shieh and L. Maleki, "Phase noise of optical interference in photonic RF systems," *IEEE Photon. Technol. Lett.,* vol. 10, no. 11, pp. 1617–1619, Nov. 1998, doi: 10.1109/68.726768.

[42] M. Kalubovilage, M. Endo, and T. R. Schibli, "Ultra-low phase noise microwave generation with a free-running monolithic femtosecond laser," *Opt. Exp.,* vol. 28, no. 17, pp. 25400–25409, 2020.

[43] D. Eliyahu, D. Seidel, and L. Maleki, "RF amplitude and phase-noise reduction of an optical link and an opto-electronic oscillator," *IEEE Trans. Microw. Theory Techn.,* vol. 56, no. 2, pp. 449–456, Feb. 2008.

[44] W. Shieh, X. S. Yao, L. Maleki, and G. Lutes, "Phase-noise characterization of optoelectronlc components by carrier suppression techniques," in *Proc. Opt. Fiber Commun. Conf.*, 1998, pp. 263–264. [Online]. Available: https://www.osapublishing.org/abstract.cfm?uri=OFC-1998-ThB6

[45] A. Hati, C. W. Nelson, and D. A. Howe, "Correlation measurements between PM and AM noise in oscillators," in *Proc. IEEE Int. Freq. Control Symp.*, 2014, pp. 1–3.

[46] L. M. Nelson, C. W. Nelson, and F. L. Walls, "Relationship of AM to PM noise in selected RF oscillators," *IEEE Trans. Ultrason., Ferroelect., Freq. Control,* vol. 41, no. 5, pp. 680–684, Sep. 1994.

[47] E. S. Ferre-Pikal and F. L. Walls, "Voltage adjustable attenuation with low 1/f noise," in *Proc. IEEE Int. Freq. Control Symp.*, 1998, pp. 186–191.

[48] K. Takagi, S. Serikawa, and T. Doi, "A method to reduce the phase noise in bipolar transistor circuits," *IEEE Trans. Circuits Syst. II Analog Digit. Signal Process.,* vol. 45, no. 11, pp. 1505–1507, Nov. 1998.

[49] A. Hati, C. W. Nelson, and D. A. Howe, "Oscillator PM noise reduction from correlated AM noise," *IEEE Trans. Ultrason., Ferroelect., Freq. Control,* vol. 63, no. 3, pp. 463–469, Mar. 2016.